J|A|C|S
ARTICLES
Published on Web 01/12/2007

Effect of Disorder on the Optically Amplified Photocatalytic Efficiency of Titania Inverse Opals

Jennifer I. L. Chen,[†] Georg von Freymann,[‡] Vladimir Kitaev,[†,§] and Geoffrey A. Ozin*,[†]

Contribution from the Materials Chemistry Research Group, Department of Chemistry, University of Toronto, 80 St. George Street, Toronto, Ontario, M5S 3H6, Canada, Institut für Nanotechnologie, Forschungszentrum Karlsruhe in der Helmholtz-Gemeinschaft, 76021 Karlsruhe, Germany, and Chemistry Department, Wilfrid Laurier University, 75 University Avenue West, Waterloo, Ontario, N2L 3C5, Canada

Received August 22, 2006; E-mail: gozin@chem.utoronto.ca

Abstract: Optically amplified photochemistry with slow photons has been realized in our previous work when a photoactive material such as TiO_2 was molded into a photonic crystal and the corresponding energy of photonic bands overlapped with the electronic excitation. While numerous applications of photonic crystals have been proposed, the real practicality depends on the extent of structural imperfection that can be tolerated before significant deterioration in the optical response deems it unrealistic to use. As a result, it is important to evaluate the amount of structural disorder that can be tolerated in inverse TiO_2 opals if they are to be used as amplified photocatalysts for photolytic degradation of organics in environmental remediation and water purification. We present a systematic study on the effect of disorder with relation to the photocatalytic efficiency of oxidizing methylene blue dye adsorbed on inverse TiO_2 opals by introducing different fractions and sizes of guest spheres into the opal template. Our results show that half of the enhancement originally achieved by the inverse opal made from monodispersed 150-nm spheres is conserved when the domain size of the host spheres remains above a critical threshold. The substitution fraction can be as high as 0.4 when the guest spheres are 1.2 times larger than the host spheres. Such a high tolerance to structural disorder provides strong support for the potential use of inverse TiO_2 opals in environmental cleanup and water treatment applications.

Introduction

The success in the development of photonic crystals in the past decade suggests their indispensable role in a wide range of fields, from optical computing and telecommunication[1] to photovoltaic[2,3] and photocatalyst.[4] The periodic modulation of the refractive index in a photonic crystal leads to a photonic stop band that forbids the propagation of light with certain frequencies. The optical response of photonic crystals is prone to any structural disorder that is intrinsic in all fabrication methods. Of the various routes for making photonic crystals, the bottom-up self-assembly of submicrometer spheres into a face-centered cubic lattice, commonly known as opal, proves to be a facile and inexpensive approach. Gravity sedimentation and convective self-assembly both yield colloidal crystals, with the latter producing single-crystal planar films over large areas with precise control over thickness.[5] The presence of defects such as stacking faults and dislocations, however, is inherent in these 3D colloidal crystals. It is known that a high monodispersity of the spheres is the key to achieving good optical response from the colloidal crystals.[6] To understand the effect of disorder on the photonic stop band, various researchers have explored the dependence of the optical properties of colloidal crystals on the polydispersity of spheres[7] or upon doping with different sizes and amounts of guest spheres.[8−10] Theoretical calculations have also been exploited to model the effect of disorder on the optical spectrum of 2D photonic crystals composed of rods.[11,12] While these studies contribute to the fundamental understanding of the effect of disorder, the actual impact of structural imperfection on a practical application of photonic crystals remains unexplored.

[†] University of Toronto.
[‡] Forschungszentrum Karlsruhe in der Helmholtz-Gemeinschaft.
[§] Wilfrid Laurier University.

(1) Joannopoulos, J. D.; Villeneuve, P. R.; Fan, S. *Nature* **1997**, *386*, 143−149.
(2) (a) Halaoui, L. I.; Abrams, N. M.; Mallouk, T. E. *J. Phys. Chem. B* **2005**, *109*, 6334−6342. (b) Nishimura, S.; Abrams, N.; Lewis, B. A.; Halaoui, L. I.; Mallouk, T. E.; Benkstein, K. D.; van de Lagemaat, J. A.; Frank, J. *J. Am. Chem. Soc.* **2003**, *125*, 6306−6310.
(3) Mihi, A.; Míguez, H. *J. Phys. Chem. B* **2005**, *109*, 15968−15976.
(4) Chen, J. I. L.; von Freymann, G.; Choi, S. Y.; Kitaev, V.; Ozin, G. A. *Adv. Mater.* **2006**, *18*, 1915−1919.
(5) Jiang, P.; Bertone, J. F.; Hwang, K. S.; Colvin, V. L. *Chem. Mater.* **1999**, *11*, 2132−2140.
(6) Li, Z. Y.; Zhang, Z. Q. *Phys. Rev. B* **2000**, *62*, 1516−1519.
(7) Rengarajan, R.; Mittleman, D.; Rich, C.; Colvin, V. *Phys. Rev. E* **2005**, *71*, 016615.
(8) Gates, B.; Xia, Y. *Appl. Phys. Lett.* **2001**, *78*, 3178−3180.
(9) Paquet, C.; Allard, M.; Gledel, G.; Kumacheva, E. *J. Phys. Chem. B* **2006**, *110*, 1605−1613.
(10) Palacios-Lidon, E.; Juarez, B. H.; Castillo-Martinez, E.; Lopez, C. *J. Appl. Phys.* **2005**, *97*, 063502.
(11) Kaliteevski, M. A.; Manzanares Martinez, J.; Cassagne, D.; Albert, J. P. *Phys. Rev. B* **2002**, *66*, 113101.
(12) Beggs, D. M.; Kaliteevski, M. A.; Abram, R. A.; Cassagne, D.; Albert, J. P. *J. Phys.: Condens. Matter* **2005**, *17*, 1781−1790.

10.1021/ja066102s CCC: $37.00

Recently, we have shown that inverse opals composed of anatase nanocrystals of TiO_2 (i-nc-TiO_2-o) can serve as efficient photocatalysts, achieving a twofold enhancement in comparison to conventional nanocrystalline TiO_2 (nc-TiO_2) when the stop-band energy is optimized with respect to the anatase absorption.[4] TiO_2 is an ideal candidate for environmental remediation and water purification owing to its photoactivity toward degrading organic pollutants and harmful microorganisms upon excitation with ultraviolet light.[13,14] By coupling light with low group velocity[15] found at the frequency edges of the stop band to the anatase absorption, a greater population of electron−hole pairs is generated and consequently higher photodegradation efficiency is achieved. It represents the first proof of principle of using slow photons in chemistry to increase the matter-radiation interaction time that results in an enhanced photocatalytic activity. The practicality of i-nc-TiO_2-o as photocatalyst in environmental cleanup and purifying water streams would depend on the level of structural disorder that can be tolerated while maintaining an optical enhancement, if large-scale i-nc-TiO_2-o is to be produced. Herein, we show a systematic study of the effect of disorder in i-nc-TiO_2-o on the photodegradation efficiency of an adsorbed organic dye methylene blue by incorporating different amounts and sizes of guest spheres into the opal template. The potential real-life performance of inverse titania opal catalysts made from submicrometer spheres with limited monodispersity is addressed.

Experimental Section

Growth of Binary Templates. The polystyrene spheres were synthesized via an emulsifier-free polymerization of styrene and styrene sulfonic acid.[16] Using scanning electron microscopy (SEM), we found that the spheres have diameters of 135, 154, 182, 209, and 243 nm (referred to as 130, 150, 180, 210, and 240 nm for simplicity). To produce the binary template films, the total volume fraction of the spheres was kept constant at 0.5 vol %. The sphere solutions were mixed in ethanol and sonicated for 5 min. Clean glass slides were then placed vertically into the solution at an ambient temperature of 35 °C to allow the self-assembly of spheres via solvent evaporation over a period of 3 to 4 days. Infiltration of the template with titanium butoxide (97%, Aldrich) was performed under low pressure with the precursor concentrations ranging from 0.7 to 1.2 vol % in anhydrous ethanol. The polystyrene−TiO_2 composite was then exposed to air plasma for 24 h to remove the polystyrene while maintaining good structural integrity, followed by calcination at a rate of 1 °C/min to 450 °C for 4 h to obtain the anatase phase. The i-nc-TiO_2-o films have thicknesses of ∼2.5 μm. The reference nanocrystalline TiO_2 was prepared as previously reported[17] or by the same deposition method as i-nc-TiO_2-o but without any template. A crushed i-nc-TiO_2-o film was also used as the reference.[4]

Characterization. SEM images were obtained using Hitachi S-5200 operating at 30 kV. Reflectance and transmission spectra were recorded using a Perkin-Elmer Lambda 900 UV−vis spectrometer.

Dye Adsorption and Photocatalysis. Films were immersed in an aqueous solution of methylene blue at 7 μM and pH of 8 in the dark to adsorb a monolayer of dye. Upon adsorption, excess dye was rinsed away and the film was dried. The samples were irradiated at half-minute intervals using an Oriel Xe-lamp (40 mW/cm^2) with a density filter that cuts off wavelengths shorter than 300 nm. Dye extinction on the film was measured spectroscopically, and the degradation of methylene blue monomer molecules was monitored through the extinction peak at 660 nm after subtracting the film background and deconvoluting the peaks using Microcal Origin. The enhancement factor was evaluated from at least two films of the same composition averaged over a total of 3−8 runs. The solid-state photocatalysis is extremely sensitive to surface contamination, and therefore all experiments were carried out with freshly prepared samples.

Results and Discussion

In our previous study, i-nc-TiO_2-o with stop-band position at 300 nm proved to be the most efficient photocatalyst owing to the slow-photon enhancement and suppression of stop-band reflection.[4] The template used in this case was 150-nm polystyrene spheres. Since the enhancement comes from the photonic structure, one would anticipate its effect to diminish with increasing structural disorder. Hence, we devised a series of experiments where the disorder was introduced by substituting different fractions of 150-nm spheres with different spheres such as 180 or 210 nm. The binary system of 150- and 180-nm spheres is denoted as $(1-x)150-x180$ where x is the mole fraction of 180-nm spheres (other binary systems follow the same notation but with different sphere sizes). We append the suffix i-nc-TiO_2-o when referring to an inverse structure. For simplicity, we refer to the size of the spherical voids in the inverse structure the same as the template sphere size. The voids are actually ∼80% of the original template size as a result of precursor polymerization-induced shrinkage during the inversion process. We first present the findings for the $(1-x)150-x180$ system with the focus on the effect of disorder on photonic strengths. The trend in the photocatalytic efficiency of $(1-x)150-x180$-i-nc-TiO_2-o is discussed in relation to the optical data of the opal templates and inverse structures. The $(1-x)150-x210$ system expands on this concept and other binary systems, such as 130−180, are investigated to address the effect of light scattering.

The optical spectra of $(1-x)150-x180$ templates show Bragg diffraction for all compositions, as seen in Figure 1a. With increasing fraction of 180-nm spheres, the stop-band position red-shifts and the transmission dips become weaker, broader, and skewed to longer wavelengths. This trend was observed in the theoretical calculation for 2D photonic crystal composed of rods with increasing deviation in the cylinder radius.[11] The plot of stop-band position as a function of x shows deviation from linear dependency (Figure 1b). At small x, the stop-band position remains relatively constant while the transmission dip decreases in magnitude. The decrease in light attenuation can be explained in terms of the decreasing domain size, as reported by Gates and Xia.[8] In their study, the optical properties of opals (230 nm) doped with smaller spheres (150 nm) were found to correlate with equations of dynamic X-ray diffraction and light scattering derived by Spry and Kosan.[18] The transmittance at

(13) Linsebigler, A. L.; Lu, G.; Yates, J. T., Jr. *Chem. Rev.* **1995**, *95*, 735−758.
(14) Fox, M. A.; Dylay, M. T. *Chem. Rev.* **1993**, *93*, 341−357.
(15) Imhof, A.; Vos, W. L.; Sprik, R.; Lagendijk, A. *Phys. Rev. Lett.* **1999**, *83*, 2942−2945.
(16) Shouldice, G. T. D.; Vandezande, G. A.; Rudin, A. *Eur. Polym. J.* **1994**, *30*, 179−183.
(17) Barbe, C. J.; Arendse, P.; Comte, P.; Jirousek, M.; Lenzmann, F.; Shklover, V.; Gratzel, M. *J. Am. Ceram. Soc.* **1997**, *80*, 3157−3171.
(18) Spry, R. J.; Kosan, D. J. *Appl. Spectrosc.* **1986**, *40*, 782−784.

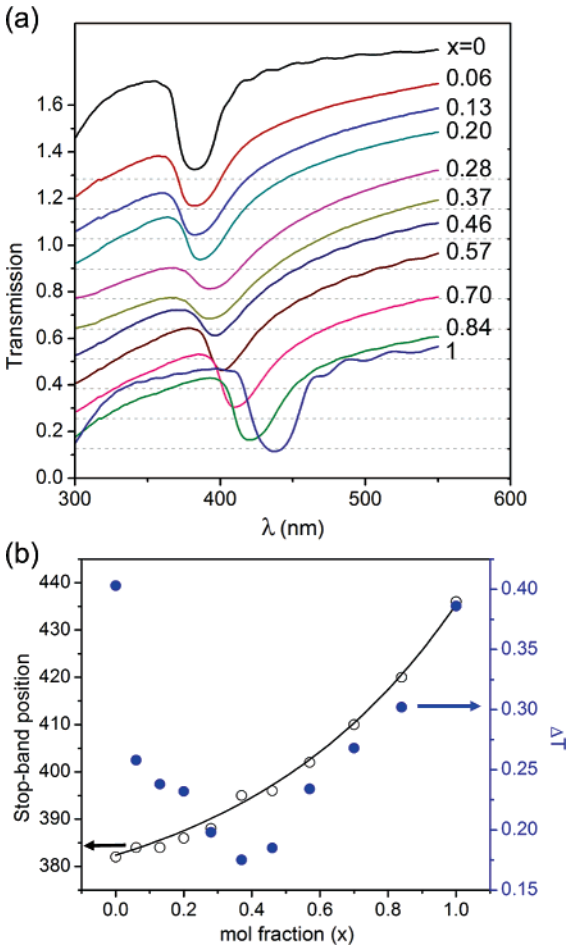

Figure 1. Transmission spectra of $(1-x)150-x180$ polystyrene opal templates (a) and trends in stop-band position and the transmission difference ($T_{\text{background}} - T_{\text{min at midgap}}$) as a function of x (b). The transmission spectra are displaced vertically for clarity, with the dashed lines marking the 0 transmission level for each spectrum.

midgap (T) depends on the "effective"thickness of the (111) packing (t), which can be calculated according to:

$$T_\lambda = [\cosh(t/t_0)]^{-2} \quad (1)$$

and

$$t_0 = [w_y(\lambda_{\min})^2 \sin\theta]/[\pi(\Delta\lambda)] \quad (2)$$

where $\lambda_{\min}$ is the wavelength of transmittance minima, θ is the angle between incident light and (111) planes (assumed to be 90°), and $\Delta\lambda$ is the bandwidth of the stop band, taken as the full width at half-maximum. The numerical factor, w_y, was determined as 0.723 in our $(1-x)150-x180$ system by solving the equation using known t for $x = 0$ and $x = 1$. Due to significant Rayleigh scattering below 400 nm, the transmissions of all compositions have been corrected to that of $x = 0$ for calculation. Figure 2 shows the effective number of (111) layers of $(1-x)150-x180$ as a function of x assuming that the diffraction originates from perfect closed-packing of either 150- or 180-nm domains. The number of (111) layers in the domain drastically decreases from 21 to 13 with the incorporation of just 6 mol % of 180-nm spheres. The domain size, however, decreases only slightly upon further doping ($0.1 < x < 0.4$) to a minimum of nine layers. It should be noted that an accurate

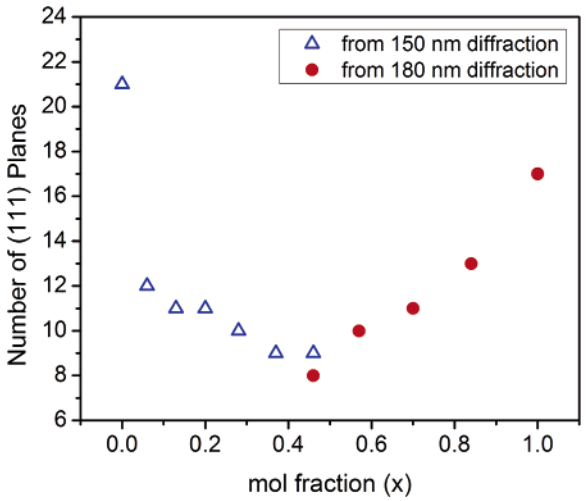

Figure 2. Relationship between the number of (111) planes and composition in $(1-x)150-x180$-i-nc-TiO_2-o. It is assumed that diffraction comes from (111) planes of closed-packing of either 150- or 180-nm spheres.

determination of the number of (111) layers for $0.4 < x < 0.6$ is not feasible as one must assume an interplanar distance for calculating the number of layers from t. It is difficult to judge whether the diffraction for $0.4 < x < 0.6$ arises from 150- or 180-nm domains or possibly from unit cells composed of the two spheres. As a result, the domain size is best approximated for compositions near the end members.

Data on the effective thickness show a more gradual decrease for 180-nm spheres doped with 150 nm (x closer to 1) than 150 nm doped with 180 nm (x closer to 0). It suggests that doping with larger spheres introduces defects that destroy long-range order much more significantly than doping with smaller spheres. It has been observed that large-host spheres form a cagelike structure around small-guest spheres without causing much change in the lattice at low doping concentrations.[9] A smaller sphere effectively occupies a position of a larger host sphere in the lattice, increasing the void space and decreasing the overall refractive index of the template. In this case, substitution with smaller spheres does not change the lattice dimension significantly as the physical contact between the larger spheres governs the unit cell lattice. The domains giving rise to (111) diffraction from 180-nm sphere-packing may well contain 150-nm spheres as point defects so that the domain size decreases more gradually. The stop band blue-shifts rapidly for compositions going away from $x = 1$ and is accompanied by a decrease in the magnitude of the transmission dip (Figure 1b) as a result of the increase in the void space.

The optical spectra of $(1-x)150-x180$ templates feature stop bands for all compositions. Several studies have concluded that a polydispersity of 6−8% causes significant deterioration in the quality and optical response of the colloidal crystal.[5,7] Some theoretical studies point out that the fundamental stop band under current investigation is less sensitive to crystal defects than the full photonic band gap between the eighth and ninth bands.[6,19] Experimentally, guest−host colloidal crystals with different diameters and fractions of guest particles incorporated in host spheres of 270 or 295 nm were investigated by Lopez and co-workers[10] and Paquet et al.,[9] respectively. Our data on

(19) Yannopapas, V.; Stefanou, N.; Modinos, A. *Phys. Rev. Lett.* **2001**, *86*, 4811−4814.

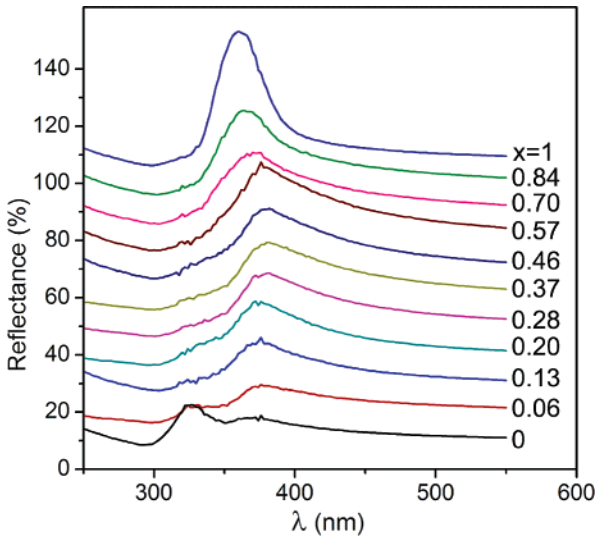

Figure 3. Reflectance spectra of $(1-x)150-x180$-i-nc-TiO_2-o in water. Spectra are displaced vertically for clarity.

$(1-x)150-x180$ is in closer agreement with the former, which reported a decrease in stop-band reflection by half when a 0.2 fraction of 350-nm spheres was incorporated into the 270-nm host template. We believe that the packing of smaller spheres (<200 nm) is even more tolerant to variations in particle size as a result of the hydration layer around the highly charged polystyrene spheres. Hence, photonic properties remain intact for all x in $(1-x)150-x180$.

The packing efficiency of binary systems of different sphere sizes at fixed volume fraction has been theoretically studied by Kansal et al.[20] According to their data, the composition for $x \approx 0.6$ in $(1-x)150-x180$ should have a packing efficiency of 65% if the spheres are randomly packed. However, the evaporative self-assembly deposition method used in our work precludes such random packing, and therefore the packing efficiency of 65% can only be regarded as a lower bound. Nonetheless, we expect the packing efficiency to decrease when binary compositions deviate from the end members as a result of more random packing of the spheres. The increase in void space of the template for compositions away from $x = 0$ or 1 was qualitatively observed experimentally when more titanium butoxide precursor was needed to completely infiltrate these templates.

While the optical response of the template is easily monitored, that of the inverse structure is difficult to observe due to the strong absorption of anatase TiO_2 at 300−350 nm. Indeed, none of the compositions other than $x = 1$ features stop-band reflection in air. However, in our previous study we showed that the stop-band reflection is more distinguishable when the samples are immersed in water. By decreasing the refractive index contrast, the stop band red-shifts to the more transparent region of TiO_2. Figure 3 shows the reflectance spectra of $(1-x)150-x180$-i-nc-TiO_2-o in water. For $x = 0$, the stop-band maximum in water is at 325 nm. It diminishes in intensity at $x = 0.06$ and becomes undetectable for $0.13 < x < 0.57$. At the other end of the composition, the stop-band red-shifts when x decreases from 1. The reflectance maximum moves from 360 to 364 to 370 for $x = 1$, 0.84, and 0.70, respectively. The red-shift in the stop-band position of the inverse structure is expected, considering that the void space in the original template increases when 150-nm spheres substitute host spheres in the 180-nm lattice. Therefore, the inverse structure with partial disorder (e.g., $x = 0.84$) has a higher filling fraction of TiO_2 than one with monodispersed spherical voids (e.g., $x = 1$). As the amount of disorder increases, the stop band of the inverse structure vanishes much more quickly than that of the template due to the difficulty in detecting photonic structure at the absorption edge of TiO_2 and the fact that structural defects and disorder may be accentuated in the inverse structure as a result of the shrinking of TiO_2 precursor.

Figure 4 shows the SEM images of various compositions of $(1-x)150-x180$-i-nc-TiO_2-o. On visual inspection, all of the inverse structures show good short-range order; little deviation from the ideal closed-packing in the (111) plane is observed. The anatase nanocrystals (~10 nm) forming the framework of the inverse structure are displayed in Figure 4b, which also illustrates how the voids from 180-nm spheres are dispersed within those of 150 nm. On the other hand, Figure 4c, where $x = 0.37$, shows that the registry between the (111) lattice planes varies within an imaging area of ~2 μm^2 as a result of the different sphere sizes. The observation on SEM images combined with optical spectra suggests that the short-range order is conserved in $(1-x)150-x180$-i-nc-TiO_2-o, but the domain size of perfect fcc-packing of 150-nm spheres decreases with increasing x. The direction of (111) for most domains remains close to perpendicular to the glass substrate since Bragg diffraction is detected for all of the $(1-x)150-x180$ templates.

The photodegradation efficiency of $(1-x)150-x180$-i-nc-TiO_2-o under white light (>300 nm) was investigated employing the same method as previously reported.[4] Namely, the photodegradation of an adsorbed monolayer of methylene blue on i-nc-TiO_2-o was monitored by UV−vis spectroscopy, and the ratio of the decay constant of i-nc-TiO_2-o to reference nanocrystalline TiO_2, termed enhancement factor (EF), was calculated as a measure of the efficiency. The adsorption of monolayer dye molecules standardizes all samples with respect to their surface area. Figure 5 shows the EF as a function of x for $(1-x)150-x180$-i-nc-TiO_2-o. For $x = 0$ (i.e., pure 150-i-nc-TiO_2-o), an EF of 2.3 was achieved and attributed to slow photons in the photonic crystal while stop-band reflection was effectively suppressed by anatase absorption. With increasing x, the overall enhancement decreases roughly by a factor of 2 from EF of 2.3 at $x = 0$ to EF of ~1.6 at $x = 0.13$ and then plateaus for $0.20 < x < 0.37$. The exponential-like decrease of EF from $x = 0$ to 0.37 can be attributed to an increase of disorder in the system, and the trend in EF follows closely with the decrease in domain size in Figure 2 since the optical properties of the template should directly correlate with the photonic properties of the inverse structure. The domain size of fcc packing of 150-nm sphereical voids remains above a critical threshold at ~10 layers, where multiple diffraction that gives rise to slow photon still dominates. Hence, the EF remains at 1.5 for x up to 0.37. A further increase in the concentration of large spheres leads to a final drop of the EF at $0.46 < x < 0.57$. This composition range may represent the breakdown point at which the clusters of 150-nm spherical voids become smaller than the critical size. Photonic effects attributed to domains formed by 150-nm voids consequently vanish.

(20) Kansal, A. R.; Torquato, S.; Stillinger, F. H. *J. Chem. Phys.* **2002**, *117*, 8212−8218.

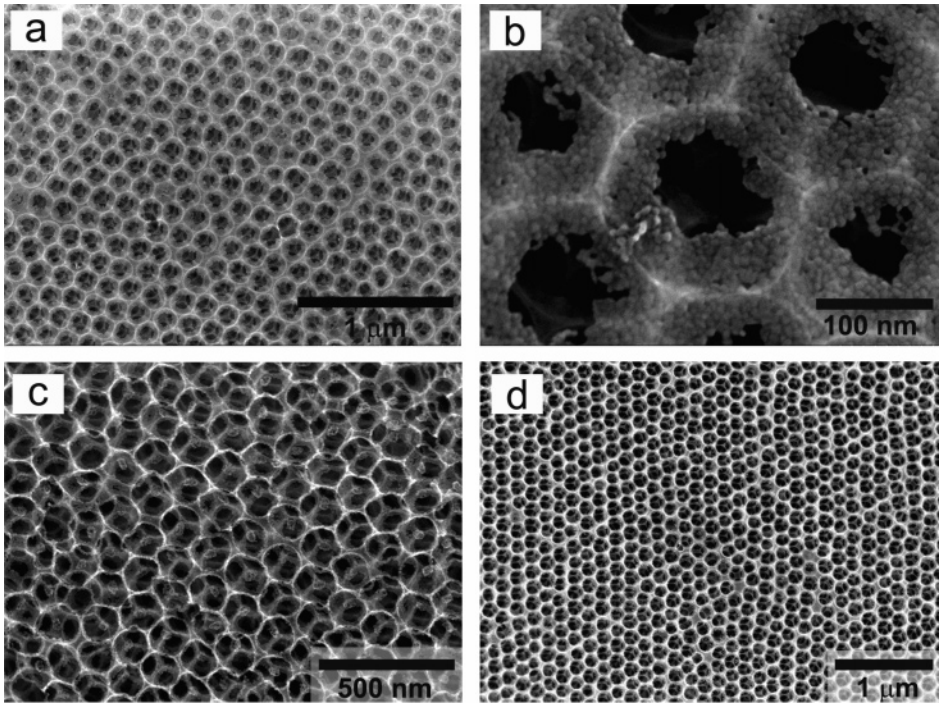

Figure 4. SEM images of $(1-x)150-x180$-i-nc-TiO_2-o with $x = 0.13$ (a and b), 0.37 (c), and 0.57 (d).

Looking at compositions near the other end member (i.e., 180-i-nc-TiO_2-o), the EF decreases with decreasing x from $x = 1$, which correlates with the increasing amount of disorder as 150-nm spheres are incorporated into 180-nm lattice. The substitution of 150-nm spheres into 180-nm lattice increases the filling fraction of TiO_2 in the inverse structure, as evidenced in the red-shift of the stop-band for $x = 0.84$ and 0.70 in comparison to $x = 1$ in Figure 3. This leads to an increase in the number of defects in the high dielectric part of the photonic crystal,[21] hence disturbing the modes that are utilized for the photodegradation. In our previous study, we showed that the EF decreases when the stop band (in air) red-shifts in the wavelength range of 300−370 nm. This is consistent with our current observations (Figure 3), as i-nc-TiO_2-o with $x = 0.84$ is less efficient than $x = 1$. The overall dependence of EF on the composition in the binary system of $(1-x)150-x180$-i-nc-TiO_2-o shows that a substantial amount of disorder can be tolerated while maintaining a respectable 50% photodegradation enhancement. This finding strongly suggests that environmental remediation and water purification using inverse TiO_2 opals can be practical and the production of the ordered photonic structure for this purpose can be rather lenient to structural defects.

Our data on the binary system of $(1-x)150-x180$-i-nc-TiO_2-o suggest that a critical domain size of ~10 layers is required for slow photons to provide at least 50% enhancement. We explored these findings further by investigating the binary system of $(1-x)150-x210$-i-nc-TiO_2-o. The larger 210-nm spheres are expected to disrupt the lattice of 150-nm spheres much more drastically than 180-nm spheres, and one would anticipate the domain size of 150-nm spherical voids to decrease at a faster rate in $(1-x)150-x210$-i-nc-TiO_2-o compared to $(1-x)150-x180$-i-nc-TiO_2-o. Figure 5 in fact shows a much faster decrease in EF without any plateau region for the binary system $(1-x)150-x210$-i-nc-TiO_2-o. The major difference in the structural disruption brought on by the 210-nm template spheres can be clearly seen in the SEM images in Figure 6. At $x = 0.10$, regions of ordered 150-nm voids interrupted by 210-nm voids can be observed (Figure 6a). Unlike the $(1-x)150-x180$-i-nc-TiO_2-o system where the void packing maintains a hexagonal arrangement and the lattice appears relatively undisturbed, the packing of the 150-nm spherical voids in $(1-x)150-x210$-i-nc-TiO_2-o rearranges upon even minor disruption by 210-nm voids. As a result, the closed-packing directions along (111) of the 150-nm

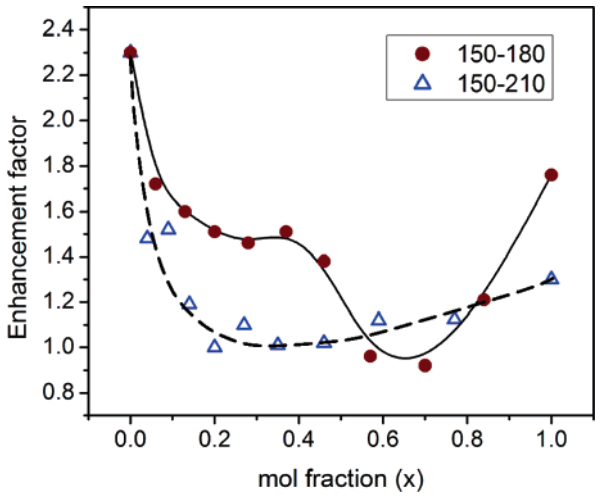

Figure 5. Enhancement factor of the photocatalytic efficiency of $(1-x)150-x180$-i-nc-TiO_2-o and $(1-x)150-x210$-i-nc-TiO_2-o as a function of composition. The solid and dashed lines are guides to the eye.

(21) Donor or acceptor defect modes can be created by adding or removing dielectric material, respectively. Doping 150-nm lattice with 180-nm spheres creates more voids in the inverse structure, while doping 180-nm lattice with 150-nm spheres increases the dielectric filling fraction. The different types of disorder may influence light localization and slow photons to a different extent. On the other hand, the sphere sizes do not differ significantly, and hence it is unlikely that defect modes inside the stop band were created. Due to complication by TiO_2 absorption, the nature of the defects could not be determined on the basis of the optical spectra. Further experimental and theoretical understanding is required to address this issue.

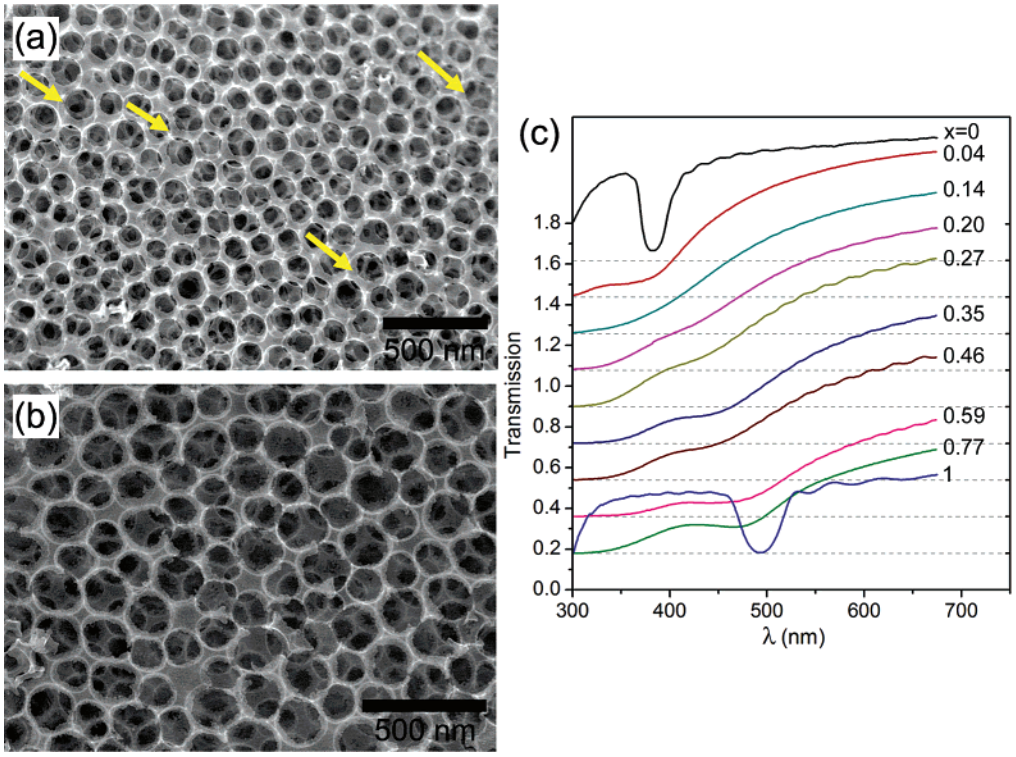

Figure 6. SEM images of $(1-x)150-x210$-i-nc-TiO_2-o with $x = 0.09$ (a) and 0.35 (b). Some aggregation of the larger 210-nm voids is observed, as indicated by the arrows in (a). Transmission spectra of $(1-x)150-x210$ polystyrene templates are displaced vertically in (c), with the dashed lines marking the 0 transmission level for each spectrum.

domains vary to a greater extent, which also correlates well with the absence of stop-band diffraction of the $(1-x)150-x210$ template even at very small x (Figure 6c). Upon close examination of a series of SEM images of low x, we noticed some phase segregation between 150 and 210 nm voids, also reported by Gates and Xia.[8] The 210-nm voids are often found to be neighboring at least one other 210-nm void, as indicated by the arrows in Figure 6a, while statistically it should not be a likely scenario at such low x. With increasing x, the packing of the spheres becomes very irregular and the packing efficiency drops greatly from 74% as can be noticed from the increased interstitial space between the voids in Figure 6b ($x = 0.35$). No short-range order of 150-nm or 210-nm voids can be seen at $x = 0.35$, and the EF effectively decreases to ~1. No stop-band reflection could be detected for any disordered $(1-x)150-x210$-i-nc-TiO_2-o in air or water, supporting the higher extent of disorder caused by the 210-nm spheres.

Since the opal templates were prepared from solutions containing a fixed total volume of the spheres, increasing x corresponds to a decrease in the volume fraction of 150-nm spheres. Consequently, it can be proposed that the enhancement is related to the density of 150-nm voids rather than the packing order. To test this hypothesis, a thicker film of $(1-x)150-x210$-i-nc-TiO_2-o with $x = 0.14$ and volume fraction of 150-nm spheres the same as $x = 0$ was prepared. The EF for the thick film was 1.14, within the experimental error of the thinner film. We therefore dismiss the density argument and conclude that structural order is the main factor responsible for the enhancement, which is also supported by the observation that EF decays at a faster rate with increasing x in $(1-x)150-x210$-i-nc-TiO_2-o than in $(1-x)150-x180$-i-nc-TiO_2-o.

It is expected that structural disorder increases light scattering within the photonic crystal. Light scattering and the corresponding longer path length of light in the material have been demonstrated to be responsible for the enhancement in dye-sensitized TiO_2 solar cells.[22−24] With increasing disorder, the $(1-x)150-x180$-i-nc-TiO_2-o becomes visibly more opaque (see Figure S1 for transmission spectra). However, none of the disordered samples in our systems showed a higher enhancement than the end members ($x = 0$ or 1), which suggests that forward scattering at the wavelengths near the TiO_2 absorption has limited contribution to the enhancement. Furthermore, if forward scattering at the disordered region was a key factor, then $(1-x)150-x210$-i-nc-TiO_2-o should have higher EF than $(1-x)150-x180$-i-nc-TiO_2-o for a given x as $(1-x)150-x210$-i-nc-TiO_2-o has a much higher degree of disorder. Conversely, it is possible that scattering from disordered regions decreases the amount of light penetrating through the material, thereby decreasing the amount of TiO_2 effectively interacting with light. Unfortunately, the interplay of photonic effect and light scattering could not be isolated in the binary systems containing 150-nm voids to clearly distinguish their contributions to the overall enhancement. On the other hand, our previous study has demonstrated that inverse opal made from 130-nm template sphere did not exhibit any photonic effect since the strong absorption of TiO_2 effectively eliminated the existence of both stop-band (extrapolated to be at 280 nm) and slow photons. A disordered inverse structure containing mostly 130-nm voids thus should serve as a good system to investigate the role of scattering from disordered regions since no photonic effect is present. We prepared an inverse structure of 130−180-i-nc-

(22) Usami, A. *Sol. Energy Mater. Sol. Cells* **1999**, *59*, 163−166.
(23) Rothenberger, G.; Comte, P.; Gratzel, M. *Sol. Energy Mater. Sol. Cells* **1999**, *58*, 321−336.
(24) Hore, S.; Nitz, P.; Vetter, C.; Prahl, C.; Niggemann, M.; Kern, R. *Chem. Commun.* **2005**, 2011−2013.

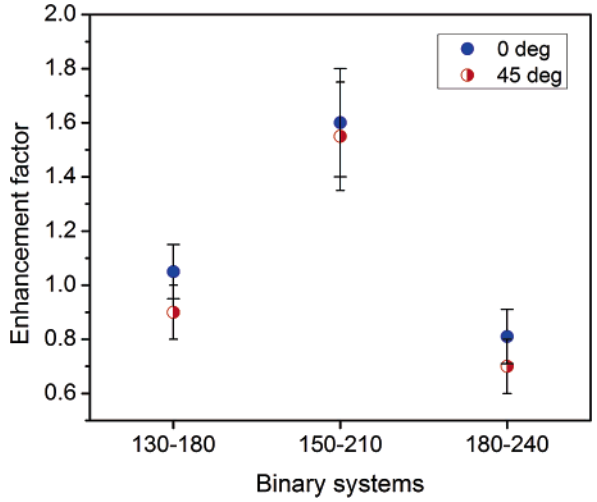

Figure 7. Enhancement factor for inverse structures of various binary systems with different sphere size combinations ($x = 0.1$) obtained at irradiation angles normal and 45° off-normal of the films.

TiO_2-o ($x = 0.1$) and found the EF to be comparable to the inverse opal of well-ordered 130-nm voids (EF of 1.05 versus 1.10). This observation, combined with the trend of EF for the $(1-x)150-x180$-i-nc-TiO_2-o and $(1-x)150-x210$-i-nc-TiO_2-o, strongly supports the idea that short-range structural order is the dominant factor in the photocatalytic enhancement. Additionally, we tested the photodegradation activity of 180−240-i-nc-TiO_2-o ($x = 0.1$), which did not show any enhancement either when compared to the reference. The EFs for irradiation normal and 45° off-normal to the films are shown in Figure 7. The photodegradation efficiency of these samples is found to be angle-independent due to the absence of photonic properties or random orientation of small 150-nm domains in the case of 150−210-i-nc-TiO_2-o, contrary to the angle-dependent behavior of the ordered inverse opals. Unlike other studies that suggest multiple scattering being favorable for increasing the path length of light, our study indicates ordered structures to be the most advantageous architecture for enhancing the photodegradation efficiency of TiO_2. Moreover, a significant enhancement (~50%) can still be achieved with x as high as 0.4 in $(1-x)150-x180$-i-nc-TiO_2-o.

Conclusions

On the basis of the systematic studies of the two binary systems $(1-x)150-x180$-i-nc-TiO_2-o and $(1-x)150-x210$-i-nc-TiO_2-o, we have demonstrated that the optical enhancement of the photocatalytic efficiency of anatase titania is governed by the domain size of close-packed 150-nm spherical voids. The domain size remains sufficiently large for photonic effects to prevail to give ~50% enhancement even when fractions as high as 0.4 of 150-nm voids were substituted by 180-nm voids. Increasing the disorder decreased the photodegradation efficiency, and thus no advantage in increasing the amount of light scattering was found in our systems. Our findings demonstrate firsthand the effect of disorder on photonic properties and how structural imperfection can impact the practical application of TiO_2-based photonic crystals. It suggests that highly monodispersed template spheres are desirable, but not absolutely necessary for practical environmental remediation or water purification using TiO_2 inverse opals. The high tolerance to structural disorder opens the door for the realistic use of colloidal photonic crystals that may be assembled from spheres of limited monodispersity or fabricated by means that are more versatile and less time-consuming, such as air-spraying or spin-coating.

Acknowledgment. G.A.O. is Government of Canada Research Chair in Materials Chemistry. J.I.L.C. and G.A.O. thank the Natural Sciences and Engineering Research Council of Canada and University of Toronto for financial support. G.v.F. acknowledges support from the Deutsche Forschungsgemeinschaft under projects FR 1671/2-1 and FR 1671/4-3 (Emmy-Noether program), and V.K. thanks Wilfrid Laurier University. We thank S. Y. Choi for guidance in the solid-state photodegradation experiment.

Supporting Information Available: Transmission spectra of $(1 - x)150 - x180$-i-nc-TiO_2-o (Figure S1). This material is available free of charge via the Internet at http://pubs.acs.org.

JA066102S